The copper centre: a transient shallow acceptor in ZnS and CdS

1992 J. Phys.: Condens. Matter 4 157

(http://iopscience.iop.org/0953-8984/4/1/025)

J. Phys.: Condens. Matter 4 (1992) 157–168. Printed in the UK

The copper centre: a transient shallow acceptor in ZnS and CdS

R Heitz, A Hoffmann, P Thurian and I Broser

Institut für Festkörperphysik, Technische Universität Berlin, Hardenbergstrasse 36, D-1000 Berlin 12, Federal Republic of Germany

Received 21 May 1991, in final form 23 July 1991

Abstract. Excitation measurements of the $^2E(D)$–$^2T_2(D)$ Cu^{2+} luminescences in ZnS and CdS crystals are presented, revealing new excitation processes of the centres. In ZnS sharp resonances observed on the low energy onset of the charge transfer band at 1.17 eV enable us to identify a transient shallow acceptor state of the Cu^{2+} centre in ZnS. An energy transfer process by photoexcited holes between Cu^{2+} and Fe^{2+} centres yields an accurate value for the deep Cu^{2+}-acceptor position in ZnS of (1.293 ± 0.005) eV. In CdS the deep Cu^{2+}-acceptor position is (1.20 ± 0.02) eV above the valence band. Additional excitation bands just below the excitonic bandgap are observed and interpreted as transitions between the conduction band and the transient shallow acceptor state. The binding energies of these state are determined to be 119 and 94 meV for ZnS and CdS, respectively. The recombination energy of the transient shallow acceptor state is transferred efficiently to the excited $^2E(D)$ state, leading to the internal Cu^{2+} luminescence.

1. Introduction

Copper is a well known luminescence activator [1] in II–VI compounds and acts as a deep acceptor strongly influencing optical and electrical properties [2]. The local binding properties of Cu centres are of special interest due to their dominant role in high T_c superconductors. Therefore, it is important to study the interaction between the Cu centres and the host material, especially the ligands. Theoretical considerations are made in the framework of LCAO methods [3]. Recently, it has been demonstrated for ZnO:Cu that scattered-wave cluster-molecular-orbital and augmented-spherical-wave bandstructure calculations are in good agreement with experimental data [4].

In optical spectra, the study of absorption and emission bands connected with the photoionization of Cu centres [5] give insight into the local binding properties. In particular, the observation of sharp resonances due to the formation of shallow bound states, as first reported in emission by Dingle [6] and in absorption by Broser *et al* [7] for ZnO:Cu, reveals information about the interaction between the impurity and the ligands [8]. In these shallow states the hole generated in the photoionization process of Cu^{2+} remains bound at the Cu^+ ion via the Coulomb interaction forming a transient shallow acceptor (TSA). Similar complexes have been observed for other 3d elements in various semiconductors (see the references in [9]) and often have been interpreted in terms of excitons deeply bound to neutral impurities. Both descriptions are possible but in general describe different situations. In the TSA complex (A^-, h_{VB})

0953-8984/92/010157+12$03.50

just the hole has to be described in the framework of effective mass theory and the dissociation products of the complex are A^- and h_{VB}. Whereas in the deeply bound exciton case (A^0, X) both the electron and the hole have to be described via effective mass theory and after dissociation the A^0 centre should remain. In principle, it is possible to determine the localization of the electron within the shallow complex by magneto-optical spectroscopy as has been demonstrated for Ni in ZnS and CdS [10], where the situations of (Ni^+, h_{VB}) and of (Ni^{2+}, X) hold, respectively. In the cases of Cu in ZnS and CdS the description TSA state is suitable, as discussed later on the basis of the binding properties. Further information about the physical nature of these TSA states yields photo-capacitive [11], electro-absorption [9], calorimetric absorption [12] and excitation [13] measurements.

The aim of the present work is the identification and characterization of the TSA states of Cu centres in ZnS and CdS. Thereby the photoluminescence excitation (PLE) spectroscopy is demonstrated as a powerful tool for the investigation of the TSA states due to its sensitivity and the often unambiguous identification of the excited states. We investigate the excitation processes of the internal $^2E(D)$–$^2T_2(D)$ luminescences of Cu^{2+}. In section 3 the role of the TSA states in the excitation processes are discussed and the photoionization energies are determined. Thereafter the energy transfer by exchange of photogenerated free holes between Cu^{2+} and Fe^{2+} centres [14] is discussed in detail. It is shown that especially from an excitation band occurring near the band edge the binding energy of the TSA state is obtained directly, without knowledge of the deep acceptor energy. The Cu centre in ZnO [6] is discussed in the framework of our results and the fine structure of the $^2E(D)$–$^2T_2(D)$ Cu^{2+} luminescence is presented.

2. Experimental results

High resolution excitation measurements were performed using a combination of a halogen or a xenon lamp with a 0.75 m double grating monochromator as light source and a double prism monochromator with a liquid nitrogen cooled Ge-diode for detection. The ZnS and CdS crystals with dimensions in the mm range were grown by the Frerich–Warminsky [15] procedure and subsequently doped in the ppm region by diffusion of Cu. The crystals contain small amounts of Fe as unintentional impurities.

Figure 1 shows the PLE spectra of the Cu^{2+} $^2E(D)$–$^2T_2(D)$ transitions in ZnS (*a*) and CdS (*b*) at low temperatures. The general features are the same in both semiconductors but for CdS the threshold energies are shifted to lower energies due to the smaller bandgap. Later we will discuss three different energy ranges of these PLE spectra in detail: the resonant excitation (R-EX) below 1 eV, the charge transfer excitation (CT-EX) above 1 eV and the near bandgap excitation (NB-EX).

2.1. The resonant excitation (R-EX)

The R-EX mechanism is the direct population of the excited $^2E(D)$ state via the $^2T_2(D)$–$^2E(D)$ absorption. In the case of CdS:Cu^{2+} two sharp resonances at 0.7744 and 0.7729 eV are observed in the excitation spectrum of the phonon sideband at 0.75 eV, corresponding to the zero phonon lines (ZPLs) in absorption [16]. In ZnS the ZPLs of the cubic (0.858 eV) and polytypic (0.844 eV) Cu^{2+} transitions, as well as their phonon sidebands can be seen in the PLE spectrum of the phonon wing at 0.765 eV. This fine structure in PLE agrees accurately with the corresponding fine structure in absorption [17]. The R-EX mechanism of Cu^{2+} in ZnS and CdS is very efficient due

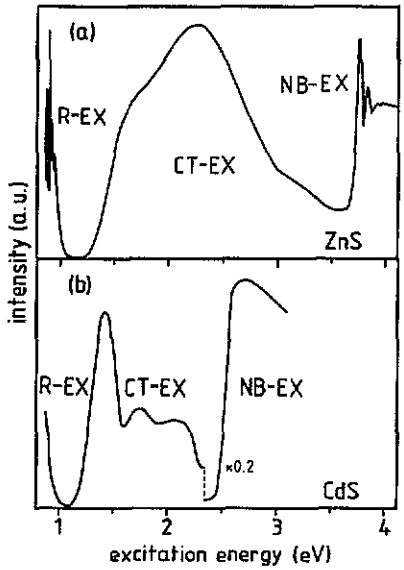

Figure 1. Photoluminescence excitation (PLE) spectra of the Cu^{2+} $^2E(D)$–$^2T_2(D)$ crystal-field transitions in ZnS (*a*) and CdS (*b*) at $T = 1.8$ K. Three different excitation processes can be distinguished: the resonant excitation (R-EX), the charge transfer excitation (CT-EX) and the near bandgap excitation (NB-EX).

to the high oscillator strengths connected with the short observed decay times of 350 and 500 ns for ZnS and CdS, respectively [18]. This is a typical behaviour in II–VI semiconductors as we also show for ZnO:Cu^{2+} in section 3.4.

2.2. The charge transfer excitation (CT-EX)

The CT-EX process is the photoionization transition $Cu^{2+} \rightarrow Cu^{+} + h_{VB}$ and the subsequent recapture of the hole, which clearly relaxes to the excited $^2E(D)$ state of Cu^{2+}. The onset of the charge transfer bands corresponds to the ionization energies of the investigated centres, which are situated at 1.3 and 1.2 eV for ZnS and CdS [11], respectively (figure 1). These threshold energies determine the positions of the Cu^{2+} $^2T_2(D)$ ground states above the edge of the valence bands (VB). Both CT-EX bands consist of three bands with maxima at 1.61, 2.25 and 3.35 eV for ZnS and 1.42, 1.74 and 2.12 eV for CdS. For ZnS the shape was explained using the density of states in the VB [19].

The CT-EX transition is of bound-to-free type and therefore no sharp structures are expected. However, a sharp excitation resonance at 1.1737 eV occurs in ZnS, see figure 2, indicating a bound-to-bound transition. Since the resonance line is observed in the excitation spectrum of the Cu^{2+} luminescence it has to be a transition to an excited Cu^{2+} state shallow above the VB which relaxes to the excited $^2E(D)$ state. The low energy onset of the CT-EX band is represented, enlarged, in figure 2. The excitation spectrum starts with a weak ZPL E_1 (FWHM = 1.7 meV) at 1.1737 eV followed by a series of phonon replicas which are superimposed on the rising structureless CT-EX band. The main phonon sidebands can be explained with three modes of the ZnS host lattice having energies of 22.4 (LA), 37.7 (TO) and 42.8 meV (LO). The energy positions and their interpretations are summarized in table 1.

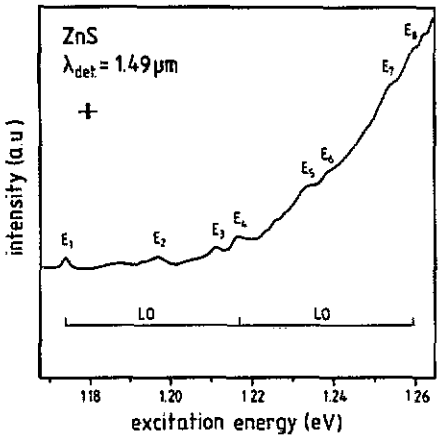

Figure 2. PLE spectrum in the CT-EX region of the Cu^{2+} $^2E(D)$-$^2T_2(D)$ luminescence in ZnS at $T = 1.8$ K.

Table 1. Energy positions and interpretations of the fine structure observed in the CT-EX band of the Cu^{2+} luminescence in ZnS, see figure 4.

	E (eV)	FWHM (meV)	ΔE (meV)	Identification
E_1	1.1737	1.7	—	NPL
E_2	1.1965	—	22.7	1+LA
E_3	1.2111	—	37.3	1+TO
E_4	1.2166	—	42.8	1+LO
E_5	1.2332	—	59.5	1+LA+TO
E_6	1.2387	—	64.9	1+LA+LO
E_7	1.2540	—	80.2	1+TO+LO
E_8	1.2595	—	85.7	1+2LO
E_9	1.2621	—	88.4	1+2LA+LO

2.3. The near-bandgap excitation (NB-EX)

NB-EX means an excitation process of the Cu^{2+} luminescence with photon energies close to the bandgap energy. As can be seen in figure 1 the NB-EX starts below the excitonic bandgap. Therefore, localized states must participate in the absorption process. While the intensity ratio of the CT-EX and the R-EX bands are constant for different crystals, the intensity of the NB-EX band changes. Copper can be stable in two charge states depending on the Fermi level [20]. The presence of Cu^+ in our crystals can be demonstrated by the increase of the Cu^{2+} absorption during additional irradiation above 2.5 eV. The intensity of the NB-EX band rises with increasing Cu^+ concentration whereas the R-EX and the CT-EX bands are connected with the presence of Cu^{2+}.

Figure 3 shows enlarged the NB-EX bands of Cu^{2+} in ZnS (*a*) and CdS (*b*) with respect to the bandgap energies of 3.834 eV and 2.582 eV, respectively. The NB-EX bands are almost structureless excitation bands starting below the excitonic bandgap and ranging up to photon energies above the bandgap. An extrapolation of the steep rises in the NB-EX bands yields onset energies of −115 meV for ZnS and −94 meV ($E \perp C$) and −83 meV ($E \parallel C$) for CdS below the respective bandgap. (The slow rise below the estimated threshold at −115 meV in the case of ZnS is also seen as onset

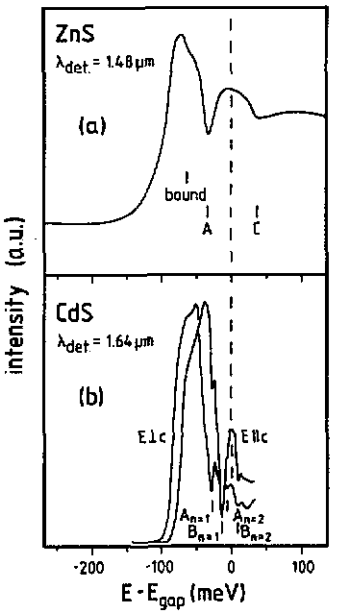

Figure 3. Photoluminescence excitation spectra of the Cu^{2+} $^2E(D)$–$^2T_2(D)$ luminescences in ZnS (a) and CdS (b) at $T = 1.8$ K. The photon energies are given with respect to the bandgap energies of 3.834 and 2.582 eV, respectively. The energy positions of the free and bound excitons are marked.

of the NB-EX of the Fe^{2+} $^3T_1(H)$–$^5E(D)$ luminescence and is therefore due to the generation of free carriers by the photoionization of Fe centres unintentionally present in the crystals.) At higher energies the typical bound and free exciton resonances are seen reducing the excitation efficiency.

For CdS we performed additional absorption and temperature dependent excitation measurements. The absorption spectra of Cu-doped samples just below the excitonic bandgap have the same shape as the excitation spectra indicating that the NB-EX in this region is dominated by a Cu-related process. At higher temperatures up to 113 K the low energy threshold of the NB-EX band as well as the free exciton minima are shifted to lower energies along with the bandgap. The energy position of the localized state with respect to the edge of the VB is temperature independent.

3. Discussion

As shown earlier it is necessary to introduce a new excited Cu^{2+} state just above the VB to understand the PLE spectra of the $^2T_2(D)$–$^2E(D)$ luminescence of Cu^{2+}. In the following sections we discuss the physical nature, the fine structure, the binding energy and the dynamical behaviour of these new Cu^{2+} states.

3.1. The shallow acceptor state

Cu^{2+} has an electronic d^9 configuration which is energetically split by the predominantly T_d crystal field of the investigated crystals in a $^2T_2(D)$ ground and a $^2E(D)$ excited state. Hence, the shallow states are not simple crystal-field states of the 3d shell of Cu^{2+}, but are clearly connected with the charge transfer processes of the Cu

centres. The Cu^+ ion, which is negatively charged in comparison with the lattice, binds the photoexcited hole by the long-range Coulomb interaction in an effective mass-like state, forming a transient shallow Cu^{2+} state. The idea of such TSA states was introduced by Dingle for the system ZnO:Cu in 1969 [6]. Since then many experimental results have shown that the formation of such acceptor and donor states is a general phenomenon connected with deep centres in II–VI [21] and probably also in III–V [12] semiconductors.

Some attempts have been made to describe theoretically the shallow states of deep centres. Recently, Mishra *et al* [4] determined these shallow states for ZnO:Cu in scattered-wave cluster-molecular-orbital and augmented-spherical-wave bandstructure calculations. Yet, in the picture of effective mass-like states we get more detailed information about the possible fine structure. Here, one carrier is strongly localized in the 3d shell of the impurity and the second is loosely bound by the Coulomb interaction in a delocalized effective mass-like state, forming shallow acceptor or donor states. The binding energies should be similar to those of closed shell acceptors or donors. In general, these states connected with open shell TMs are not stable but form an excited state of the centre. The dynamical processes will be discussed later. The incomplete 3d shells of the TM ions with their residual spin and orbital angular momenta interact with the loosely bound carrier through the non-spherical Coulomb and the exchange interaction. The eigenstates of the centre have to be calculated in the product space of the 3d electrons and the effective mass-like carrier, leading to a rich fine structure in the shallow state. This model is only practicable if one of the carriers is strongly localized in the 3d shell, as for ZnS:Cu and CdS:Cu, where the deep acceptor levels lie almost in the middle of the bandgap. Otherwise, the deeply bound carrier would experience a noticeable admixture of host band wavefunctions also. Probably, this is the case for ZnO:Cu, where the binding (localization) energy of the hole is larger than for the electron.

The Cu-associated shallow acceptor state is the simplest one among those associated with TM centres. In its monovalent charge state copper has a closed shell configuration ($3d^{10}$) without any spin or orbital momentum, transforming like Γ_1. The irreducible representations of the acceptor ground states are given by the direct product [22]

$$\Gamma_{(Cu^+,h)} = \Gamma_{Cu^+} \times \Gamma_{ac} \times \Gamma_{VB}.$$

where $\Gamma_{(Cu^+,h)}$, Γ_{Cu^+}, Γ_{ac} and Γ_{VB} are the irreducible representations of the TSA Cu states, the Cu^+ state, the acceptor state and the VB at the Γ-point, respectively. Cu^+ and the $n = 1$ state of an acceptor transform like Γ_1. Therefore, the ground state of the shallow acceptor transforms like the VB at the Γ-point of the Brillouin zone.

In ZnS with its zinc blende structure we observe one ZPL at 1.1737 eV in the CT-EX spectrum (figure 2), which corresponds to the dipole allowed transition between the Γ_7 ground state of Cu^{2+} and the Γ_8 ground state of the TSA state. The phonon sideband shown in figure 2 agrees with those observed for the system ZnS:Ni [23] which concerns phonon energies and intensity ratios, indicating an almost identical phonon coupling in both cases. Sokolov *et al* [22] postulated that the phonon coupling is dominated by the strongly localized carrier. Therefore, the 3d cores of Ni^+ with its $^2T_2$ configuration and Cu^+ with its A_1 configuration are supposed to interact with different local phonons. Since this is in contradiction to our experimental observations, we propose that the phonon coupling is dominated by the bound hole.

In CdS a corresponding ZPL in the CT-EX spectrum has not yet been observed, but the NB-EX spectra give information about the fine structure of the TSA state. In CdS the VB is formed mainly by the 3p orbitals of the sulphur ions. The hexagonal crystal-field and the spin–orbit interaction lead to a threefold Γ_9, Γ_7 and Γ_7 splitting of the VB. At the Γ-point the energy split between the highest Γ_9 and Γ_7 bands amounts to 16 meV. The NB-EX spectra for $E \parallel C$ and $E \perp C$ show two different low energy thresholds separated by 11 meV (figure 3(*b*)). The polarizations of the NB-EX bands are consistent with a Γ_7–Γ_7 ($E \parallel C$) and a Γ_7–Γ_9 ($E \perp C$) transition, holes from the A and the B VBs are involved in the TSA state, respectively. The energy separation of 11 meV is less than the 16 meV splitting of the VB, the reason being a delocalization of the hole wavefunctions in the k-space due to its spatial localization [8].

3.2. The binding energy

The determination of the binding energy of the TSA state is difficult due to its transient nature. In general one has to estimate the energy position of the deep Cu-acceptor with an accuracy better than the binding energy of the TSA state in the order of 0.1 eV. The energy position of the deep Cu-acceptor determines the CT-EX band, but it is difficult to get an exact value for the energy threshold, because the low energy onset is superimposed by transitions into the TSA state and its phonon replicas. To overcome this problem it is necessary to employ a detector for free holes as it is given by the $Fe^{3+}(^4T_1(G)$–$^6A_1(S))$ luminescence in the investigated ZnS crystals [14]. In the region of its low energy threshold around 1.3 eV the excitation of the Fe^{3+} luminescence is dominated by an energy transfer via photoexcited holes from Cu^{2+} to Fe^{2+} centres. The intensity of the Fe^{3+} luminescence is proportional to the concentration of the excited free holes. Assuming that the main source of holes is the $Cu^{2+} \rightarrow Cu^{+} + h_{VB}$ CT process the onset of the Fe^{3+} excitation is proportional to the Cu charge transfer. Thus we can determine the ionization energy of the Cu^{2+} centre. The following relation should hold for the absorption cross section (σ) of such a photoionization transition of a deep TM acceptor near the threshold energy (E_{ion}) [24]

$$\sigma \simeq v^g (h\nu - E_{ion})^{3/2}$$

where $|g| = 1$ depends on the wavefunction of the isoelectronic TM impurity. Within a small energy range near the ionization energy, $\sigma^{2/3}(h\nu)$ and therefore $I^{2/3}(h\nu)$ should be linear with zero at the ionization energy. Figure 4 shows a $I^{2/3}$ plot of the Fe^{3+} excitation spectrum. A linear extrapolation yields an ionization energy of the deep Cu acceptor in ZnS at $T = 1.8$ K of

$$E_{ion}(Cu^{2+}(^2T_2(D))) = (1.293 \pm 0.005)\ \text{eV}.$$

Thus, the ionization energy of the shallow acceptor state of the Cu centre in ZnS is

$$E_{ion}(Cu^{+}, h_{VB}) = (119 \pm 5)\ \text{meV}.$$

In addition, it is possible to check the TSA binding energy via the threshold of the NB-EX spectrum. The NB-EX mechanism can easily be explained in the framework of the TSA Cu state. The presence of Cu^{+} in the investigated crystals leads to transitions between the ionized acceptor and the CB

$$Cu^{+} + h\nu \rightarrow (Cu^{+}, h_{VB}) + e_{CB}.$$

Subsequently the TSA state relaxes as described earlier causing the infrared Cu^{2+} luminescence. The binding energy of the shallow acceptor is given by the energy difference between the low energy onset of the NB-EX spectra and the bandgap. This onset at -115 meV (figure 3) agrees very well with the previously determined (119 ± 5) meV. At higher energies above the excitonic bandgap the excitation efficiency decreases due to reflection losses and competitive decay channels [25]. The excitation minima at 3.800 and 3.871 eV correspond in their energy positions with the free A and C excitons (figure 3(*a*)). The continuous excitation up to photon energies above the bandgap is astonishing, since the penetration depth of the exciting light becomes very small compared with the crystal thickness. As the luminescence of Cu centres is a volume effect, the excitation is connected with the fast diffusion of excitation energy by free carriers or reabsorption of luminescence.

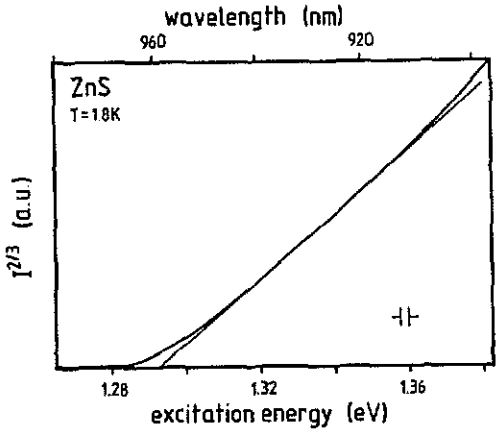

Figure 4. The low energy onset of the Fe^{3+} PLE spectrum [14] in a $I^{2/3}$ plot.

In analogy to ZnS the NB-EX spectrum of CdS:Cu, figure 3(*b*), also yields the binding energy of the hole in the TSA state, which amounts to

$$E_{\text{ion}}(\text{Cu}^+, \text{h}) = (94 \pm 5) \text{ meV}.$$

An extrapolation of the steep rise in the charge transfer band (figure 1(*b*)) yields a photoionization energy of (1.20 ± 0.02) eV for Cu^{2+} in CdS. Thus, the ZPLs should be located around 1.11 eV, which coincides with the low energy threshold of the CT-EX band.

Figure 5 gives the energy schemes of the Cu^{2+} centres in ZnS and CdS in the 'hole' picture. Thereby it is possible to combine the one-electron description of the photoionization transition and the many-electron description of the intra-shell processes of Cu^{2+} considering the photoionization process

$$\text{Cu}^{2+} + h\nu \rightarrow \text{Cu}^+ + \text{h}_{\text{VB}}.$$

Thereby Cu^+ is related to the bottom of the conduction band, and the energy levels of Cu^{2+} are positioned corresponding to their photoionization energies, respectively [11]. The excitation and recombination processes as discussed earlier are represented by arrows. The TSA state of Cu^{2+} above the VB is denoted as (Cu^+, h_{VB}). The ionization energies of the shallow and deep Cu-acceptor states are summarized in table 2.

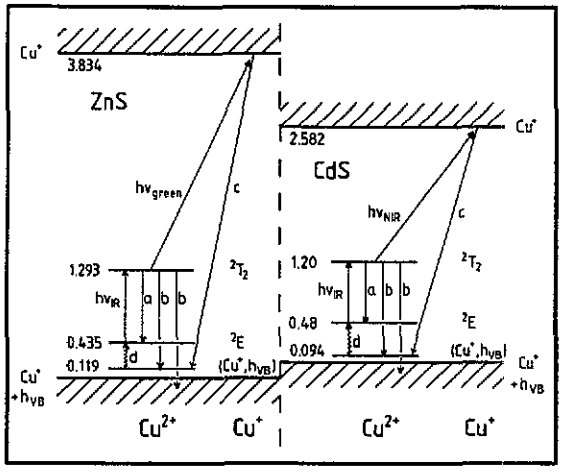

Figure 5. Schematic hole pictures of isolated Cu^{2+} centres in ZnS and CdS, the many-electron states of Cu^{2+} are given by the photoionization processes $Cu^{2+} \rightarrow Cu^{+} + h_{VB}$. The observed luminescence and excitation transitions are represented by arrows: (*a*) R-EX, (*b*) CT-EX and (*c*) NB-EX. The non-radiative relaxation process of the hole from the (Cu^{+}, h_{VB}) state to the excited $^2E(D)$ state is indicated by arrow d. $h\nu_{green}$ in ZnS and $h\nu_{IR}$ in CdS correspond to DAP recombination processes with Cu^{2+} as deep acceptor. The energies are given in eV.

Table 2. Bandgap energies (E_{gap}), ionization energies of the Cu^{2+} centres (E_{ion}), binding energies of the hole (E_{hole}) and localization energies of the electron (E_{elec}) in the shallow acceptor states (Cu^{+}, h) in different II–VI semiconductors.

(eV)	E_{gap}	E_{ion}	E_{hole}	E_{elec}
ZnS	3.834	1.293	0.119	2.541
CdS	2.582	1.20	0.094	1.38
ZnO	3.438	3.25[a]	0.39	0.19[a]

[a] From [33].

The binding energies for ZnS:Cu and CdS:Cu are smaller than those of closed shell acceptors [26]. The reduction of the binding energies can be explained with a hybridization of the Cu 3d states and the ligand orbitals. The negative effective charge of the Cu^{+} centre is then 'smeared out' over the next ligands leading to a decrease in the electrostatic interaction with the hole. The degree of this smearing depends on the localization of the deep bound electron scaling with its Bohr radius [27]. The localization energy of the electron corresponds to the energy difference between the Cu ground state and the nearest band, see table 2.

3.3. Transition probabilities

In this section we discuss the Cu^{2+} transitions as far as they occur in the excitation spectra, see figure 5. The excitation spectroscopy allows us to investigate the underlying recombination channels. Starting with Cu^{2+} in its $^2T_2(D)$ ground state the R-EX process as well as the luminescence show that the $^2E(D)$ state recombines radiatively. Optical transitions between the $^2E(D)$ and the $^2T_2(D)$ state are allowed by symmetry, the radiative lifetimes are 350 and 500 ns for ZnS and CdS, respectively [18]. Transitions to the Γ_8 ground state of the shallow acceptor are also symmetry

allowed but the poor overlap between the Cu 3d orbitals and the effective mass-like hole state reduce the transition probability. This transition is more than three orders of magnitude weaker than the R-EX transition, corresponding to a radiative lifetime in the ms range. The strong lattice relaxation connected with the different charge distributions in the Cu^{2+} states and the shallow acceptor state results in fast radiationless recombination to the excited $^2E(D)$ state. The ZPL E_1 in ZnS has an almost Lorentzian lineshape. Therefore, from its FWHM of 1.7 meV, a lifetime in the sub-ps region can be estimated, which is caused by the non-radiative transition d. The energy differences are small related to the LO-phonon energies for radiationless recombination by LO emission [28]. The high probability of optical transitions to the VB (CT-EX band) is due to the large density of VB states. Cu^+ centres are very effective traps for free holes with capture cross sections [29] of more than 10^{-15} cm^2. They are captured by the long-range Coulomb interaction forming the shallow acceptor state.

The Cu^+/Cu^{2+} charge transfer process is much less likely to be due to the d-like and s-like character of the Cu states and the CB, respectively. Although Cu^+ is present in the investigated crystals and the

$$Cu^+ + h\nu \rightarrow Cu^{2+}(^2E(D)) + e_{CB}.$$

charge transfer transition leads to excited Cu^{2+} centres we did not observe the corresponding transitions in the PLE spectra. It is superimposed by the more intense Cu^{2+}/Cu^+ CT-EX process. The NB-EX mechanism is efficient due to the p-like character of the TSA state. The TSA state relaxes leading to the Cu^{2+} crystal-field luminescence. The subsequent capture of the electron by the Cu^{2+} centre is slow due to the low capture cross section [29] of about 10^{-21} cm^2 and should result in luminescence bands below 2.54 and 1.38 eV in ZnS and CdS, respectively. However, in general the electrons are captured by donors first and subsequently donor–acceptor pair (DAP) recombination with Cu centres as deep acceptors occur [30].

3.4. ZnO:Cu

In ZnO the TSA state decays radiatively to the $^2T_2(D)$ Cu^{2+} ground state causing the prominent green emission [6]. In contrast to ZnS and CdS the energy distance from the shallow state to the excited $^2E(D)$ state of 2.14 eV is too large for efficient radiationless recombination. Accordingly, no internal Cu^{2+} luminescence has been observed under excitation in the visible spectral region. However, this luminescence has been reported for R-EX excitation at 0.859 eV [18] and is also observed under UV excitation above the bandgap, see figure 6, which is in agreement with recently reported cathodoluminescence results [31]. The polarized emission at 0.7167 eV agrees with the $\Gamma_4(^2E)$–$\Gamma_{5,6}(^2T_2)$ absorption [32] of Cu^{2+} and shows the isotope splitting of about 135 μeV at higher resolution, see insert of figure 6. The emission lines at 0.7088 and 0.7051 eV are unpolarized. The energy shifts of 7.9 and 11.6 meV correspond to TA-phonons of the ZnO lattice. These transitions are also observed in absorption spectra at 77 K. Therefore, they can also be further ZPLs as proposed by Dietz [32], but in this case they should be polarized.

ZnO:Cu has been the model system for the TSA state [6], but with respect to our results one has to question this interpretation. The model of the transient shallow acceptor state assumes the additional electron to be in the 3d shell of the Cu impurity and the hole delocalized in its vicinity. In contrast, for the TSA state in ZnO the binding energy of the hole is about twice as large as the localization energy of the

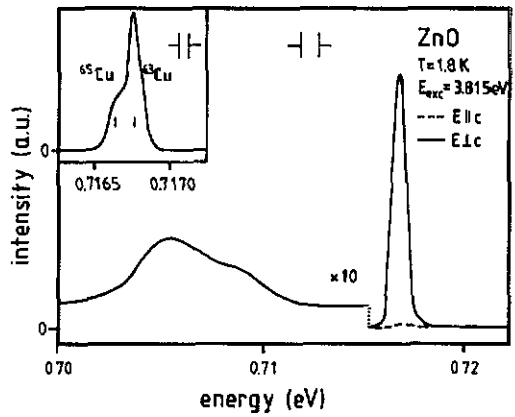

Figure 6. Luminescence spectrum of a Cu-doped ZnO crystal under optical excitation at 3.815 eV ($T = 1.8$ K). The insert shows the ZPL at higher resolution, the isotope splitting is marked.

electron due to the energy position of the Cu^{2+} ground state [33], see table 2. The observed shallow state should be in between the two extreme cases of the TSA state (Cu^{+},h) and the isoelectronic bound electron–hole pair (Cu^{2+},e,h). The magnetic field dependence of the shallow state can be explained with a shallow acceptor like state [8], whereas the radiative lifetime [34] of 250 ns and the absence of the radiative recombination to the ^{2}E(D) state indicate a deeply bound electron–hole pair.

4. Summary and conclusions

In the present paper we reported high resolution PLE measurements of Cu^{2+} transitions in ZnS and CdS. The new fine structure in the CT-EX band (ZnS) as well as the new NB-EX bands are explained in the framework of TSA Cu states. In these states the holes are bound to the negatively charged Cu^{+} ions by the Coulomb interaction. The new experimental results enable us to determine the binding energies as (119 ± 5) and (94 ± 5) meV in ZnS and CdS, respectively. The fine structures of the shallow acceptor states are dominated by the valence band structure at the centre of the Brillouin zone. We observed only one Γ_8 state in ZnS and a Γ_9 and a Γ_7 state separated by 11 meV in CdS. The CT-EX bands yield the Cu^{2+} ground states (1.293 ± 0.005) and (1.20 ± 0.02) eV above the edges of the valence bands in ZnS and CdS, respectively. The more accurate value for ZnS is based on the observed energy transfer between Cu^{2+} and Fe^{2+} by free holes.

Excitation spectroscopy is an efficient tool to obtain information about recombination mechanisms. For ZnS and CdS the Cu^{+} centres are efficient traps for free holes due to the formation of the TSA states. Subsequently, the shallow state relaxes to the excited ^{2}E(D) Cu^{2+} state. Especially, the NB-EX bands are the main excitation mechanism in the UV and blue spectral region.

Acknowledgments

The authors wish to thank Dr R Broser for supplying the crystals. We are grateful to

H Over for some of the experimental measurements in CdS:Cu. This work has in part been supported by the Deutsche Forschungsgemeinschaft.

References

[1] Garlick G F J and Dumbleton M J 1954 *Proc. Phys. Soc.* B **67** 442;
Weakleam H A 1962 *J. Chem. Phys.* **36** 2117
[2] Broser I and Broser R 1956 *J. Physique Rad.* **8**, 9 791
Broser I, Scherz U and Wöhlicke M 1970 *J. Lumin.* **1/2** 39
[3] Ferreira L G and de Siqueira M L 1986 *Phys. Rev.* B **34** 5315
Müller G M and Scherz U 1980 *Phys. Rev.* B **21** 5717
[4] Mishra K C, Schmidt P C, Johnson K H, DeBoer B G, Berkowitz J K and Dale E A 1990 *Phys. Rev.* B **42** 1423
[5] Broser I and Schulz H-J 1961 *J. Electrochem. Soc.* **108** 545
[6] Dingle R 1969 *Phys. Rev. Lett.* **23** 579
[7] Broser I, Germer R, Schulz H-J and Wisznewski K 1978 *Solid-State Electron.* **21** 1597
[8] Robbins D J, Herbert D C and Dean P J 1981 *J. Phys. C: Solid State Phys.* **14** 2859
[9] Sokolov V I and Kikoin K A 1989 *Sov. Sci. Rev.* A **12** 149
[10] Heitz R, Hoffmann A and Broser I 1990 *Frühjahrstagung de DPG in Regensburg*
Hoffmann A, Heitz R and Broser I unpublished
[11] Grimmeiss H G, Kullendorff N and Broser R 1981 *J. Appl. Phys.* **52** 3405
[12] Juhl A, Hoffmann A and Binnberg D 1987 *Appl. Phys. Lett.* **50** 1292
[13] Bishop S G, Robbins D J and Dean P J 1980 *Solid State Commun.* **33** 119
[14] Hoffmann A, Heitz R and Broser I 1990 *Phys. Rev.* B **41** 5806
[15] Broser I and Broser-Warminsky R 1950 *Deutsches Patentamt* Patentschrift 814193
[16] Hoffmann A, Broser I, Thurian P and Heitz R 1990 *J. Cryst. Growth* **101** 532
[17] Broser I, Maier H and Schulz H-J 1965 *Phys. Rev.* A **6** 2135
[18] Broser I, Hoffmann A, Heitz R and Thurian P 1991 *Proc. ICL 1990 J. Lumin.* **48/49** 693
[19] Broser I, Franke K-H and Schulz H-J 1967 *Proc. II–VI Semiconducting Compounds 1967* 81
[20] Schulz H-J 1963 *Phys. Status Solidi* **3** 485
[21] Robbins D J 1981 *J. Lumin.* **24/25** 137
[22] Sokolov V I and Surkova T P 1987 *Sov. Phys.-Solid State* **29** 1689
[23] Noras J M and Allen J W 1980 *J. Phys. C: Solid State Phys.* **13** 3511
[24] Allen J W 1969 *J. Phys. C: Solid State Phys.* **2** 1077
[25] Pantke K-H, Over H and Broser I 1990 *Phys. Status Solidi* b **159** 437
[26] Landolt-Börnstein 1982 *Semiconductors* vol 17b II–VI and I–VII, ed O Madelung (Berlin: Springer)
[27] Fleurov V N and Kikoin K A 1982 *Solid State Commun.* **42** 353
[28] Robbins D J and Dean P J 1978 *Adv. Phys.* **27** 499
[29] Hemila S O and Bube R H 1967 *J. Appl. Phys.* **38** 5258
[30] Suzuki A and Shionoya S 1971 *J. Phys. Soc. Japan* **31** 1455;
Patil S G and Woods J 1971 *J. Lumin.* **4** 231
[31] Kimpel B M and Schulz H-J *Phys. Rev.* B at press
[32] Dietz R E, Kamimura H, Sturge M D and Yariv A 1963 *Phys. Rev.* B **132** 1559
[33] Mollwo E, Müller G and Wagner P 1973 *Solid State Commun.* **13** 1283
[34] Baumert R, Broser I, Pohl U W and Sange B 1985 *J. Phys. C: Solid State Phys.* **18** 4767